

**SIMULATION AND CHARACTERIZATION OF
CHARGE CARRIER TRANSPORT IN ORGANIC
SEMICONDUCTOR TRANSISTOR**

UMAR FARUK BIN SHUIB



PERPUSTAKAAN
UNIVERSITI MALAYSIA SABAH
UMS

**THIS IS SUBMITTED IN PARTIAL
FULFILLMENT FOR THE DEGREE OF MASTER
OF ENGINEERING**

**FACULTY OF ENGINEERING
UNIVERSITI MALAYSIA SABAH
2017**

UNIVERSITI MALAYSIA SABAH

THESIS VERIFICATION STATUS FORM

TITLE: **SIMULATION AND CHARACTERIZATION OF CHARGE CARRIER TRANSPORT IN ORGANIC SEMICONDUCTOR TRANSISTOR**

DEGREE: **MASTER OF ENGINEERING (ELECTRICAL AND ELECTRONIC ENGINEERING)**


I hereby, **UMAR FARUK BIN SHUIB**, academic session of 2012-2016; declare that this bachelor thesis is stored in the Library of Universiti Malaysia Sabah with conditions as follows :-

1. This thesis is the property of Universiti Malaysia Sabah.
2. Universiti Malaysia Sabah library to make copies for educational purposes only.
3. Library of Universiti Malaysia Sabah to make copies of the thesis for academic exchange.
4. Please tick (/)

Confidential (Contains information that degree of safety or interests of Malaysia as enshrined in Secret Act 1972)

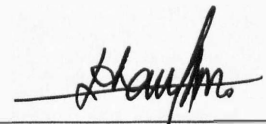
Limited (Contains restricted information as specified by the organization / institution where the research was conducted)

Not Limited


UMAR FARUK SHUIB
(MK1221029T)

Verified by, **NURULAIN BINTI ISMAIL**
LIBRARIAN
UNIVERSITI MALAYSIA SABAH

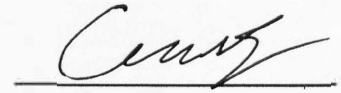

(Librarian Signature)


(Dr. Khairul Anuar Mohamad)
Supervisor

DECLARATION

I hereby declare that the work in this thesis is my own except for quotations and summaries which have been duly acknowledged.

11 January 2017



Umar Faruk Bin Shuib

MK1221029T



UMS
UNIVERSITI MALAYSIA SABAH

CERTIFICATION

NAME : **UMAR FARUK BIN SHUIB**

MATRIC NO. : **MK1221029T**

TITLE : **SIMULATION AND CHARACTERIZATION OF CHARGE
CARRIER TRANSPORT IN ORGANIC SEMICONDUCTOR
TRANSISTOR**

DEGREE : **MASTER OF ENGINEERING (ELECTRICAL AND
ELECTRONIC ENGINEERING)**

VIVA DATE : **16 JUNE 2016**



DECLARED BY;
UNIVERSITI MALAYSIA SABAH

1. SUPERVISOR

Dr. Khairul Anuar Mohamad

Signature

A handwritten signature in black ink, appearing to read 'Khairul Anuar Mohamad', is written over a horizontal line.

ACKNOWLEDGEMENT

The completion of the thesis has been made possible by many other people, who have supported me throughout the project. Hence, I would also like to take this opportunity to record my appreciation to those who are directly and indirectly involved in writing this thesis.

My special gratitude goes to my supervisor Dr. Khairul Anuar Mohamad who has shared his time and effort in guiding me towards the success of this work. Lots of moral supports and appreciation done from my supervisor who given me his constructive comments and suggestions to complete this research and help make the project finish smoothly. Special thanks to the Ministry of Education Malaysia as this research was supported financially through the Fundamental Research Grant Scheme (FRGS0306-TK-1/2012).

I would like to begin by thanking my father, Shuib Bin Dirwan, for his constant, unconditional love and support. For my late mother, Maznah Binti Abd Ghaffar, no words are sufficient to describe my late mother's contribution to my life. I owe every bit of my existence to her. This thesis is dedicated to her memory. I have been lucky to receive tremendous affection from several members in my extended family. Their support and encouragement has been instrumental in my overcoming several hurdles in life. Last but not least, my appreciation goes to each and every person who had encouraging me during my study.

Umar Faruk Bin Shuib

11 January 2017

ACKNOWLEDGEMENT

The completion of the thesis has been made possible by many other people, who have supported me throughout the project. Hence, I would also like to take this opportunity to record my appreciation to those who are directly and indirectly involved in writing this thesis.

My special gratitude goes to my supervisor Dr. Khairul Anuar Mohamad who has shared his time and effort in guiding me towards the success of this work. Lots of moral supports and appreciation done from my supervisor who given me his constructive comments and suggestions to complete this research and help make the project finish smoothly. Special thanks to the Ministry of Education Malaysia as this research was supported financially through the Fundamental Research Grant Scheme (FRGS0306-TK-1/2012).

I would like to begin by thanking my father, Shuib Bin Dirwan, for his constant, unconditional love and support. For my late mother, Maznah Binti Abd Ghaffar, no words are sufficient to describe my late mother's contribution to my life. I owe every bit of my existence to her. This thesis is dedicated to her memory. I have been lucky to receive tremendous affection from several members in my extended family. Their support and encouragement has been instrumental in my overcoming several hurdles in life. Last but not least, my appreciation goes to each and every person who had encouraging me during my study.

Umar Faruk Bin Shuib

11 January 2017

ABSTRACT

The main objective of this research is to investigate the charge transport in organic devices by simulating the 2-D design structure of the device using TCAD tools. As organic transistors are preparing to make improvements towards flexible and low cost electronics applications, an accurate models and simulation methods were demanded to predict the optimized performance and circuit design. The extraction and analysis of the transistor parameters from the electrical characterization of the 2-D organic semiconductor device were done to learn the behavior of the device itself. The characterization can describe the behavior of the transistor in the linear and saturation region, which is determining the drain current for any applied voltages. One of the important parameter for organic transistor devices is field effect mobility, the extraction of gate voltage dependence and the contact effects. Acknowledging the contact effect is very significant since it contribution on the device performance. Varied temperature research on organic transistor also has been used to characterize charge transport. There few common established model for charge transport in organic semiconductors because the exposed on thermally activated charge transport which is activation energies. Thus, the analysis of the effect of contact resistance and thermal activation energy of organic transistor also been investigated. The contact resistance obtained then fitted into the linear region equation for modified mobility, μ_{mod} which obtain higher mobility than those obtained from the common linear region mobility model, proves that contact resistance should be considered while estimating the mobility. The observed temperature dependence of mobility can be explained by empirical MNR while there is an inverse relationship between E_a and μ_{MN} . The μ_0 reveals that lower temperature region has lower mobility than the higher temperature region.

ABSTRAK

SIMULASI DAN PENCIRIAN PENGANGKUTAN PEMBAWA CAS DALAM TRANSISTOR SEMIKONDUKTOR ORGANIK

Objektif utama kajian ini adalah untuk menyiasat angkutan cas dalam peranti organik oleh simulasi reka bentuk struktur 2-D peranti menggunakan alat-alat TCAD. Sejak akhir ini, transistor organik telah mengalami penambahbaikan ke arah aplikasi elektronik fleksibel dan kos rendah, mempunyai model yang tepat dan kaedah simulasi telah digunakan untuk meramalkan prestasi dan reka bentuk litar untuk dioptimumkan. Pengekstrakan dan analisis parameter transistor dari pencirian elektrikal di dalam 2-D peranti semikonduktor organik telah dijalankan untuk mengetahui bagaimana keputusan peranti itu sendiri. Pencirian boleh menggambarkan keadaan transistor di kawasan linear dan tepu, yang menentukan arus salir bagi mana-mana voltan digunakan. Salah satu parameter yang penting untuk peranti transistor organik adalah mobiliti efektif medan elektrik, pengekstrakan pada kerbergantungan voltan dan kesan kontak. Ia telah pon diakui bahawa kesan kontak mempunyai hubungan yang sangat ketara kepada prestasi peranti. Penyelidikan suhu pada pelbagai tahap untuk transistor organik juga telah digunakan untuk mencirikan pengangkutan caj. Terdapat beberapa model yang dihasilkan untuk pengangkutan caj dalam semikonduktor organik kerana terdedah kepada pengangkutan caj yang diaktifkan secara haba yang merupakan tenaga pengaktifan bagi sesuatu transistor tersebut. Oleh itu, analisis kesan rintangan kontak dan tenaga pengaktifan haba transistor organik juga telah disiasat. Rintangan kontak yang diperolehi telah diaplikasikan ke dalam persamaan kawasan linear untuk mobiliti yang diubah suai, μ_{mod} , yang mendapatkan mobiliti yang lebih tinggi berbanding yang diperolehi dari linear model mobiliti kawasan tepu yang sama, membuktikan bahawa rintangan kontak perlu dipertimbangkan semasa menganggarkan mobiliti. Pergantungan pada suhu juga diperhatikan pada mobiliti dapat dijelaskan oleh model MNR yang menunjukkan terdapat hubungan songsang antara E_n dan μ_{MN} . Pendapatan nilai μ_0 juga telah mendedahkan bahawa kawasan suhu yang lebih rendah mempunyai mobiliti lebih rendah daripada suhu yang lebih tinggi.

TABLE OF CONTENTS

	Page
TITLE	i
DECLARATION	ii
CERTIFICATION	iii
ACKNOWLEDMENT	iv
ABSTRACT	v
<i>ABSTRAK</i>	vi
TABLE OF CONTENTS	vii
LIST OF TABLES	xi
LIST OF FIGURES	xiii
LIST OF ABBREVIATIONS	xvii
LIST OF SYMBOLS	xviii
LIST OF APPENDIX	xxi
CHAPTER 1: INTRODUCTION	1
1.1 Project Background	1
1.2 Problem Statement	2
1.3 Objectives	3
1.4 Project Scope	3
1.5 Outline	3
CHAPTER 2: LITERATURE REVIEW	5
2.1 Introduction	5
2.2 Basic Field-Effect Transistors (FETs) Operation	5
2.3 Organic Semiconductors	9
2.3.1 Oligoacenes	10
2.4 Operating Mode of The Organic Transistor	13
2.5 Conductance	14
2.5.1 Ohmic Conduction	15
2.5.2 Poole-Frenkel	16
2.5.3 Tunnelling	18

2.5.4	Hopping Transport	18
2.6	Simulation in Organic Transistor	20
2.6.1	Literature on Simulation of Organic Transistor	20
2.7	Factors Influencing the Charge Mobility	23
2.7.1	Molecular Packing	23
2.7.2	Crystal Disorder	25
2.7.3	Temperature	26
2.8	Contact Resistance	28
2.9	Chapter Summary	29
CHAPTER 3: METHODOLOGY		31
3.1	Chapter Overview	31
3.2	Research Methodology Flow	31
3.3	Extraction Using IEEE Standard Test Method	33
3.3.1	Device Structure	33
3.3.2	Analytical Model	34
3.4	Sentaurus Structure Editor	37
3.4.1	Sentaurus	38
3.4.2	Advantages of Sentaurus Tools	39
3.5	Sentaurus Simulation and Mobility	40
3.5.1	Simulation Design	40
3.5.2	Mobility	42
3.6	Temperature Dependence	43
3.6.1	Physical Structure and TCAD Simulation	43
3.7	Temperature Dependence with Meyer-Nedel Rule Model	45
3.7.1	TCAD Simulation Design	45
3.8	Characterization and Extraction	45
3.8.1	I-V Characterization	45
3.8.2	Mobility Extraction	46
3.8.3	Contact Resistance Extraction	47
3.8.4	The Contact Resistance Model	49
3.9	Disordered Crystalline Materials and The Meyer-Nedel Rule	50
3.9.1	Meyer-Nedel Rule for Effective Mobility	51

REFERENCES	102
APPENDIX A: MATLAB CODE FOR CHANNEL LENGTH	110
APPENDIX B: SENTAURUS TOOL	113
APPENDIX C: SENTAURUS CODE FOR TEMPERATURE DEPENDENT	127
APPENDIX D: PUBLICATIONS	133



UMS
UNIVERSITI MALAYSIA SABAH

LIST OF TABLES

	Page
Table 2.1 : Literature list of research using pentacene as the organic material for organic transistor	12
Table 2.2 : Literature comparison of simulation of organic transistor	22
Table 2.3 : Literature list of research on temperature dependence mobility	27
Table 2.4 : Literature list on contact resistance of organic transistors	29
Table 3.1 : Parameters and characteristics for organic transistor	34
Table 3.2 : Device configuration	40
Table 3.3 : Parameters for TCAD simulation	42
Table 3.4 : Device configuration	43
Table 4.1 : Drain current on gate voltage of -0.5 V and -3 V for 50 μm channel length	57
Table 4.2 : Drain current on gate voltage of -0.5 V and -3 V for 10 μm channel length	58
Table 4.3 : Drain current on gate voltage of -0.5 V and -3 V for 5 μm channel length	59
Table 4.4 : Drain current on different drain voltage for each channel length	61
Table 4.5 : Mobility on gate voltage of -0.5 V and -3 V for 10 μm channel length	62
Table 4.6 : Drain current on gate voltage of -40V for 10 μm , 20 μm and 30 μm channel length	66
Table 4.7 : Drain current on gate voltage of -40V for 50 μm , 80 μm and 100 μm channel length	67
Table 4.8 : Drain current on gate voltage range from -10V to -40V for 10 μm channel length	68
Table 4.9 : Linear and saturation mobility for 10 μm channel length	69

Table 4.10 :	Parasitic resistance for 10 μm channel length	71
Table 4.11 :	Linear and mobility with contact resistance at different gate voltage	73
Table 5.1 :	Drain current with range of gate voltage from -10 V to 40 V for temperature 300 K	76
Table 5.2 :	Drain current with range of gate voltage from -10 V to 40 V for temperature 3250 K	77
Table 5.3 :	Drain current with range of gate voltage from -10 V to 40 V for temperature 350 K	78
Table 5.4 :	Parasitic resistance for temperature 300, 325 and 350 K	81
Table 5.5 :	Linear mobility and at mobility with contact resistance in different temperature	82
Table 5.6 :	Drain current with range of gate voltage of -20, -40 and -60V for temperature 70 K	84
Table 5.7 :	Drain current with range of gate voltage of -20, -40 and -60V for temperature 100 K	85
Table 5.8 :	Drain current with range of gate voltage of -20, -40 and -60V for temperature 140 K	86
Table 5.9 :	Drain current with range of gate voltage of -20, -40 and -60V for temperature 180 K	87
Table 5.10 :	Drain current with range of gate voltage of -20, -40 and -60V for temperature 220 K	88
Table 5.11 :	Drain current with range of gate voltage of -20, -40 and -60V for temperature 260 K	89
Table 5.12 :	Drain current with range of gate voltage of -20, -40 and -60V for temperature 300 K	90
Table 5.13 :	Activation energy for temperature range between 140-70 K and 300-180 K at different gate voltage	95
Table 5.14 :	$\ln\mu$ value for certain activation energy	96

Table 4.10 :	Parasitic resistance for 10 μm channel length	71
Table 4.11 :	Linear and mobility with contact resistance at different gate voltage	73
Table 5.1 :	Drain current with range of gate voltage from -10 V to 40 V for temperature 300 K	76
Table 5.2 :	Drain current with range of gate voltage from -10 V to 40 V for temperature 3250 K	77
Table 5.3 :	Drain current with range of gate voltage from -10 V to 40 V for temperature 350 K	78
Table 5.4 :	Parasitic resistance for temperature 300, 325 and 350 K	81
Table 5.5 :	Linear mobility and at mobility with contact resistance in different temperature	82
Table 5.6 :	Drain current with range of gate voltage of -20, -40 and -60V for temperature 70 K	84
Table 5.7 :	Drain current with range of gate voltage of -20, -40 and -60V for temperature 100 K	85
Table 5.8 :	Drain current with range of gate voltage of -20, -40 and -60V for temperature 140 K	86
Table 5.9 :	Drain current with range of gate voltage of -20, -40 and -60V for temperature 180 K	87
Table 5.10 :	Drain current with range of gate voltage of -20, -40 and -60V for temperature 220 K	88
Table 5.11 :	Drain current with range of gate voltage of -20, -40 and -60V for temperature 260 K	89
Table 5.12 :	Drain current with range of gate voltage of -20, -40 and -60V for temperature 300 K	90
Table 5.13 :	Activation energy for temperature range between 140-70 K and 300-180 K at different gate voltage	95
Table 5.14 :	$\ln\mu$ value for certain activation energy	96

LIST OF FIGURES

	Page
Figure 2.1 : Schematic energy diagram of a metal-organic interface. E_{VAC} : vacuum energy level, E_F : Fermi energy of metal, E_{HOMO} : energy of the band edge of the semiconductor.	6
Figure 2.2 : Schematic diagram of the energy distribution of localized electronic states in the energy gap between the highest occupied molecular orbital (HOMO) and lowest unoccupied molecular orbital (LUMO) bands.	7
Figure 2.3 : Localized and delocalized states and density of states, $Z(E)$ for amorphous semiconductors. Note the band tails, which are caused by the localized states.	8
Figure 2.4 : Structure of organic semiconductors based on small molecules.	9
Figure 2.5 : Chemical structures of a) oligoacenes (n=2, 3, 4, 5 represent naphthalene, anthracene, tetracene and pentacene, respectively), b) rubrene, c) triisopropylsilyl (TIPS) pentacene.	10
Figure 2.6 : Geometry of a rubrene molecule (a) in the gas phase (b) and in the crystalline phase.	11
Figure 2.7 : A schematic diagram of one plane of a pentacene crystal.	12
Figure 2.8 : Three dimensional view of a top contact bottom gate organic transistor.	13
Figure 2.9 : Showing the three region of operation, which is intrinsic, saturation and freeze-out, for temperature dependence of the hole density.	16
Figure 2.10 : Illustration of the large variation in mobilities measured for various TTF derivatives.	24
Figure 2.11 : Charge carrier mobilities as a function of temperature in pentacene crystal from 60 to 350 K.	26

Figure 3.1 :	Flowchart of research approach.	32
Figure 3.2 :	Cross-sectional view of a general top contact bottom gate transistor.	33
Figure 3.3 :	Sentaurus Structure Editor interface.	37
Figure 3.4 :	Top contact device structure.	40
Figure 3.5 :	Top contact device mesh structure for channel length 100 μm .	40
Figure 3.6 :	Top contact device mesh structure for channel length 10 μm .	44
Figure 3.7 :	(a) Equivalent circuit of a TFT without contact resistance and (b) circuit of TFT including contact resistance.	47
Figure 3.8 :	Schematic of the general form of the MNR in Arrhenius plots.	51
Figure 3.9 :	Arrhenius plots of the experimentally determined μ_{FE} of a bottom contact OFET with (symbols) and the simulated μ_{FE} values (lines) for $V_{GS} = 10\text{V}$ and $V_{GS} = 15\text{V}$.	53
Figure 4.1 :	Output characteristics for 50 μm channel length.	57
Figure 4.2 :	Output characteristics for 10 μm of channel length.	58
Figure 4.3 :	Output characteristics for 5 μm of channel length.	59
Figure 4.4 :	Output characteristics for drain source current at -3V gate voltage for each channel length.	60
Figure 4.5 :	Mobility versus gate voltage for channel length 10 μm at gate voltage range of -0.5 to -3V.	62
Figure 4.6 :	Channel length dependency of sub-threshold slope and on/off current ratio.	63
Figure 4.7 :	Sentaurus simulation and output characteristics for different channel length vary from 10 μm to 100 μm at gate voltage of -40V.	66

Figure 4.8 :	Output characteristics for 10 μm of channel length at drain voltage range of 0V to -40V.	68
Figure 4.9 :	Mobility vs. V_{GS} in linear region ($V_{DS} = -6\text{V}$) and saturation region ($V_{DS} = -40\text{V}$).	69
Figure 4.10 :	Plot of $R_{ON}W$ vs. Channel length. The value of gate voltages varies from -5 to -40V in steps of -5V.	70
Figure 4.11 :	Plot of R_p vs. Gate Voltage for Channel Length of 10 μm .	71
Figure 4.12 :	Linear Mobility, μ_{linear} (blue triangle) and Mobility with contact resistance, μ_{mod} (red triangle).	72
Figure 5.1 :	Output characteristics from TCAD simulation for temperature at 300 K with V_{DS} varies from 0 V to - 40 V and V_{GS} from -10 V to - 40 V.	76
Figure 5.2 :	Output characteristics from TCAD simulation for temperature at 325 K with V_{DS} varies from 0 V to - 40 V and V_{GS} from -10 V to - 40 V.	77
Figure 5.3 :	Output characteristics from TCAD simulation for temperature at 350 K with V_{DS} varies from 0 V to - 40 V and V_{GS} from -10 V to - 40 V.	78
Figure 5.4 :	Maximum I_{DS} for temperature 300 K, 325 K and 350 K.	79
Figure 5.5 :	Shows the $I_{DS} - V_{GS}$ for each temperature at constant $V_{DS} = -4\text{V}$.	79
Figure 5.6 :	R_p versus temperature for 300, 325 and 350 K.	80
Figure 5.7 :	Mobility versus temperature on 300, 325 and 350 K for mobility with contact resistance and linear mobility.	82
Figure 5.8 :	The output characteristics of the device shown at different gate voltages at 70 K	84
Figure 5.9 :	The output characteristics of the device shown at different gate voltages at 100 K.	85
Figure 5.10 :	The output characteristics of the device shown at different gate voltages at 140 K.	86

Figure 5.11 :	The output characteristics of the device shown at different gate voltages at 180 K.	87
Figure 5.12 :	The output characteristics of the device shown at different gate voltages at 220 K.	88
Figure 5.13 :	The output characteristics of the device shown at different gate voltages at 260 K.	89
Figure 5.14 :	The output characteristics of the device shown at different gate voltages at 300 K.	90
Figure 5.15 :	The transfer characteristics at different temperatures in the linear region for $V_{DS} = -2$ V.	91
Figure 5.16 :	The transfer characteristics at different temperatures in the saturation region for $V_{DS} = -60$ V.	91
Figure 5.17 :	Mobility in the linear region versus V_{GS} at different temperature from 70 to 300 K.	92
Figure 5.18 :	Arrhenius plot of linear mobility at different gate voltages for each temperature.	93
Figure 5.19 :	V_{GS} dependent E_a evaluated using the data from Figure 5.19 in two different ranges of T .	94
Figure 5.20 :	Plot of μ_0 versus E_a using the data from Figure 5.19	96

LIST OF ABBREVIATIONS

OFETs	-	Organic field effect transistors
FETs	-	Field effect transistors
HOMO	-	Highest occupied molecular orbital
LUMO	-	Lowest unoccupied molecular orbital
PF	-	Poole-Frenkel
TOF	-	Time of flight
TCAD	-	Technology computer-aided design
OTFTs	-	Organic thin film transistors
ANN	-	Artificial neural network
TFT	-	Thin film transistor
MNR	-	Meyer-Neldel Rule
MTR	-	Multiple trapping and release
TLM	-	Transmission line method
MOSFET	-	Metal-oxide semiconductor field effect transistor
FinFET	-	Fin Field Effect Transistor
FDSOI	-	Fully depleted silicon on insulator
HEMTs	-	High-electron-mobility transistors
HBTs	-	Heterojunction bipolar transistors
GUI	-	Graphical user interface

LIST OF SYMBOLS

E_F	-	Fermi energy
E_{HOMO}	-	Energy of the band edge of semiconductor
E_{vac}	-	Vacuum energy level
ϕ_B	-	Schottky barrier of height
ϕ_M	-	Metal work function
V_D	-	Drain voltage
V_G	-	Gate voltage
V_{TH}	-	Threshold voltage
k_B	-	Boltzman constant
T	-	Temperature
W	-	Channel Width
L	-	Channel length
V_{DS}	-	Source drain voltage
I_{DS}	-	Drain source current
V_{GS}	-	Gate source voltage
C_i	-	Capacitance of the insulator
μ	-	Mobility
G	-	Ratio of current and voltage
σ	-	Material parameter conductivity
A	-	Area of the device
d	-	Length of the device
J	-	Drift current
μ_p	-	Diffusion mobility

D_p	-	Diffusion coefficient
μ_0	-	Zero-field mobility
γ	-	Poole-Frenkel fitting parameter
ε	-	Electric field
μ_i	-	Intrinsic mobility
Δ	-	Zero activation energy
T_{eff}	-	Effective temperature
T_0	-	Temperature fitting parameter
F	-	Magnitude of the electric field
$\mu(E)$	-	Field dependent mobility
β	-	Electron Poole-Frenkel factor
E	-	Electric field
R_C	-	Contact resistance
V_C	-	Contact region at the channel
T_{MN}	-	Isokinetic temperature
E_{MN}	-	Meyer-Neldel energy
E_a	-	Variable activation energy
μ_{MN}	-	Meyer-Neldel mobility
μ_{FE}	-	Field effect mobility
ε_i	-	Dielectric permittivity
d_i	-	Dielectric thickness
Q_o	-	Surface density
$Q_g(x)$	-	Surface density of the carriers in the accumulation layer
$V_s(x)$	-	Ohmic drop
$V(x)$	-	Potential on coordinate x

$W(x)$	-	Width of the depletion region
R_s	-	Parasitic source
R_d	-	Drain contact resistance
R_p	-	Parasitic resistance
R_{ch}	-	Channel resistance
μ_{linear}	-	Linear mobility
μ_{mod}	-	Modified contact resistance mobility



UMS
UNIVERSITI MALAYSIA SABAH

LIST OF APPENDIX

	Page
Appendix A : MATLAB CODE FOR CHANNEL LENGTH	6
Appendix B : SENTAURUS TOOL	7
Appendix C : SENTAURUS CODE FOR TEMPERATURE DEPENDENT	7
Appendix D : PUBLICATIONS	8



UMS
UNIVERSITI MALAYSIA SABAH

CHAPTER 1

INTRODUCTION

1.1 Project Background

As the organic semiconductors were introduced on the early years of its discovery, the structure of organic semiconductor is proven compatible with thin film transistor (TFT) but have limitation on the organic material which have low mobility in device performances of initial device (Calveti *et al.*, 2005). Many techniques were introduced to improve organic semiconductor performance especially on the charge-carrier mobility and pulling the interest of industrial group board into research programs on organic transistor (Li and Kosina, 2005). Even though the carrier mobility of organic materials makes their performance characteristics lag behind traditional inorganic semiconductors by a thousand times or more, the organic semiconductors offer easier low-temperature processing than silicon, resulting in lower cost semiconductors with highly tunable properties (Johnson, 2010).

As the interest getting bigger, the physical dimensions of organic semiconductor device were scaling down. For example, the channel length in organic thin film transistor is getting shorter, which can lead to substantial deviations of the device such as short channel effects (Li and Kosina, 2005). It is estimated that the carriers move at a much higher velocity and produced very high current (Brütting, 2006). Hence, an accurate extraction of certain type of organic transistor model parameters is benefits from modelling and circuit simulation and could be a give significantly higher performance value as it will be more reliable according to the specified configuration (Weis *et al.*, 2013).